

Supporting information

From monomeric complexes to double-stranded helicates constructed around *trans*- TiO_4N_2 motifs with intramolecular inter-ligand hydrogen-bonding interactions.

Georges Khalil, Laurent Barloy, Nathalie Kyritsakas, Pierre Mobian, Marc Henry

$[\text{Ti}(\text{L}^1)_2(\text{Pyr})_2]$

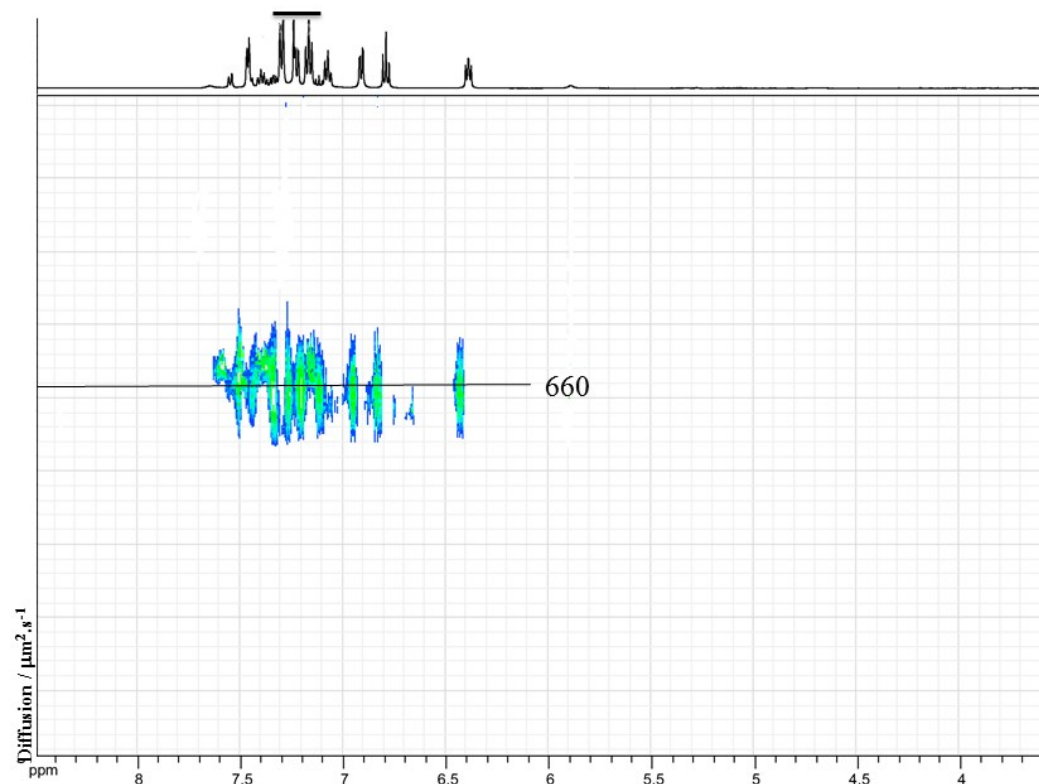


Fig 1: ¹H NMR DOSY map (CDCl_3) of $[\text{Ti}(\text{L}^1)_2(\text{Pyr})_2]$

[Ti(L¹)₂(DHA)₂]

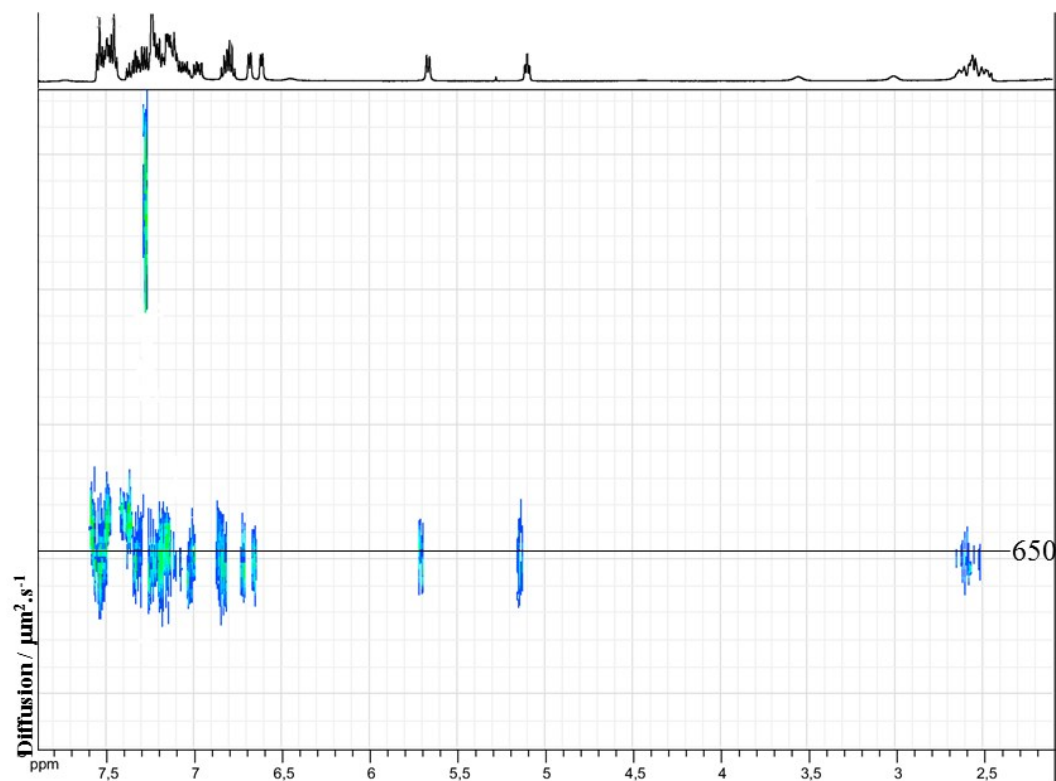


Fig 2: ¹H NMR DOSY map (CDCl₃) of [Ti(L¹)₂(DHA)₂]

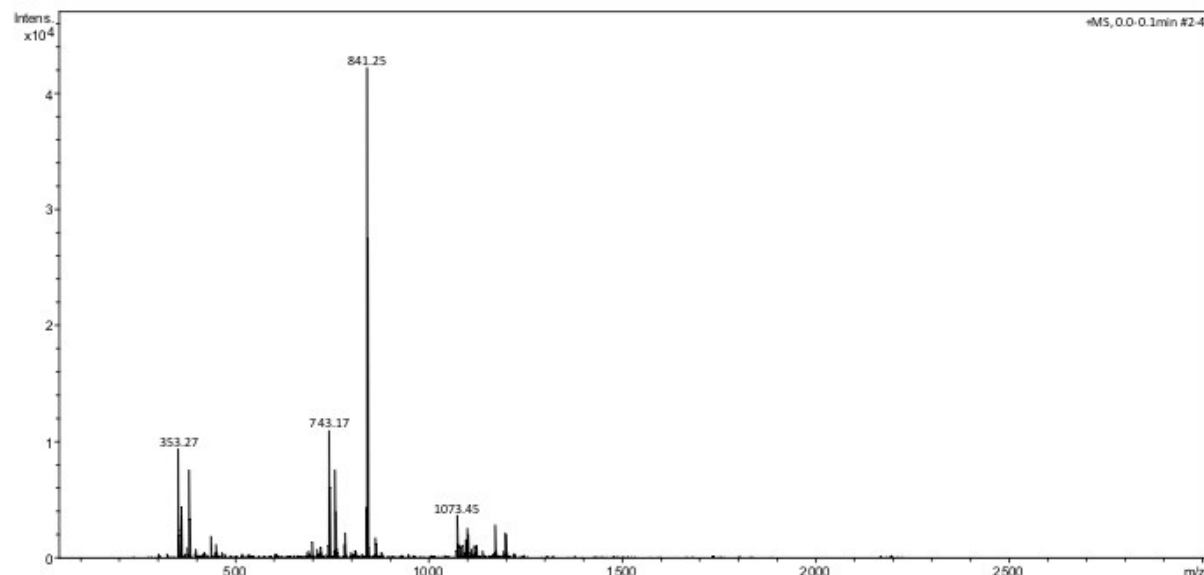


Fig 3: ES-MS spectrum of [Ti(L¹)₂(DHA)₂].

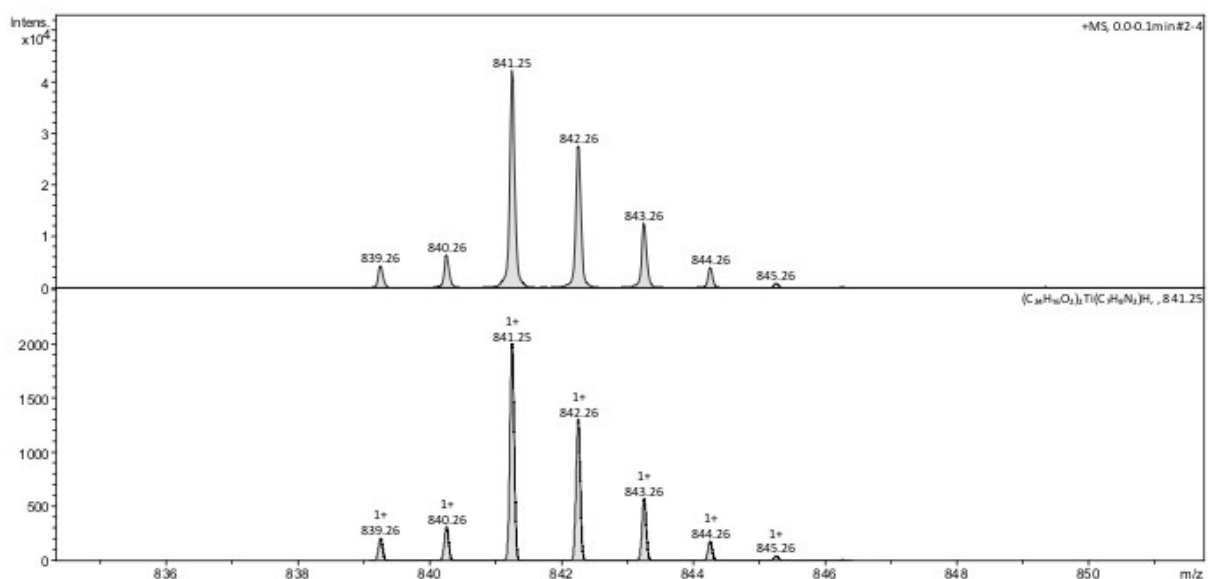


Fig 4: ES-MS spectrum of $[\text{Ti}(\text{L}^1)_2(\text{DHA})_2]$. Enlargement at $m/z = 841$. Experimental peak (top) and simulated peak for $[\text{Ti}(\text{L}^1)_2(\text{DHA})_2] + \text{H}^+$ (bottom).

$[\text{Ti}(\text{L}^1)_2(\text{MePyr})_2]$

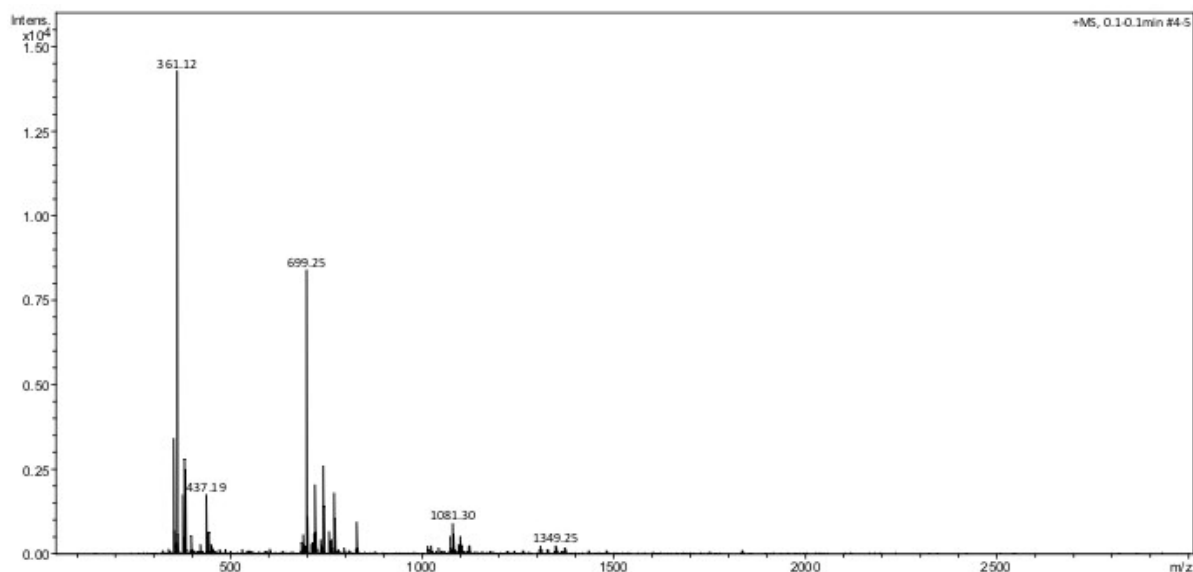


Fig 5: ES-MS spectrum of $[\text{Ti}(\text{L}^1)_2(\text{MePyr})_2]$.

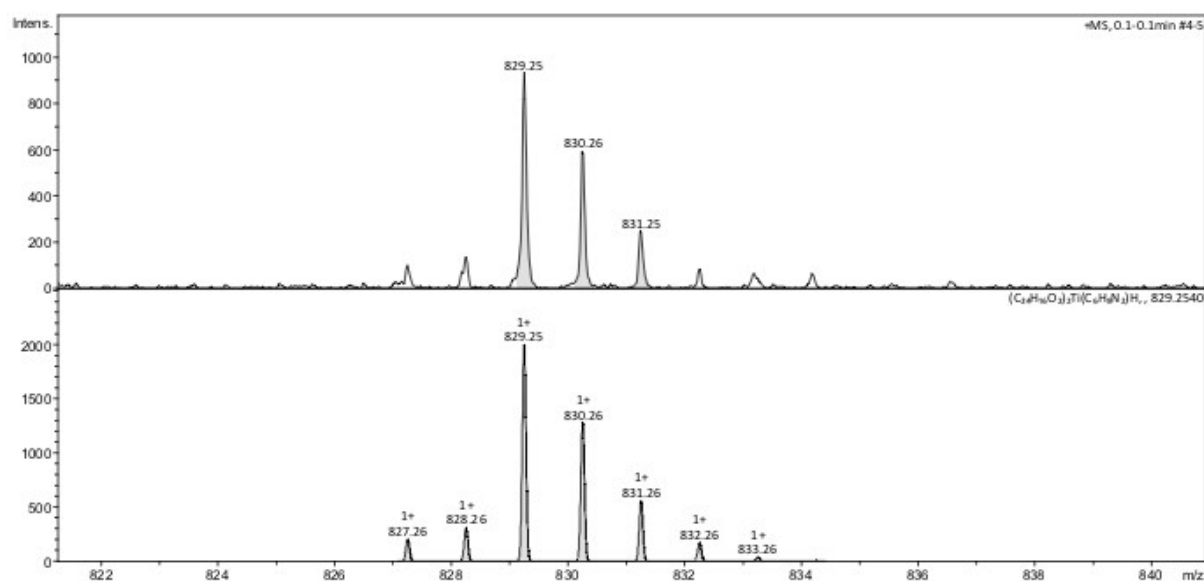


Fig 6: ES-MS spectrum of $[\text{Ti}(\text{L}^1)_2(\text{MePyr})_2]$. Enlargement at $m/z = 829$. Experimental peak (top) and simulated peak for $[\text{Ti}(\text{L}^1)_2(\text{MePyr})_2] + \text{H}^+$ (bottom).

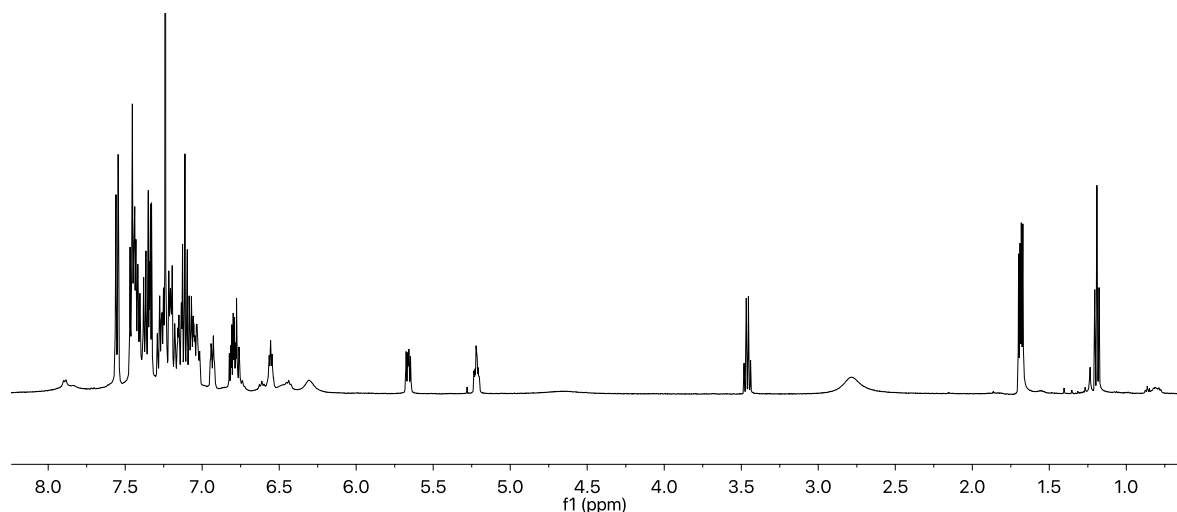


Fig 7: ^1H NMR spectrum (CDCl_3) of $[\text{Ti}(\text{L}^1)_2(\text{MePyr})_2]$ crystals.

$[\text{Ti}(\text{L}^2)_2(\text{DHA})_4]$

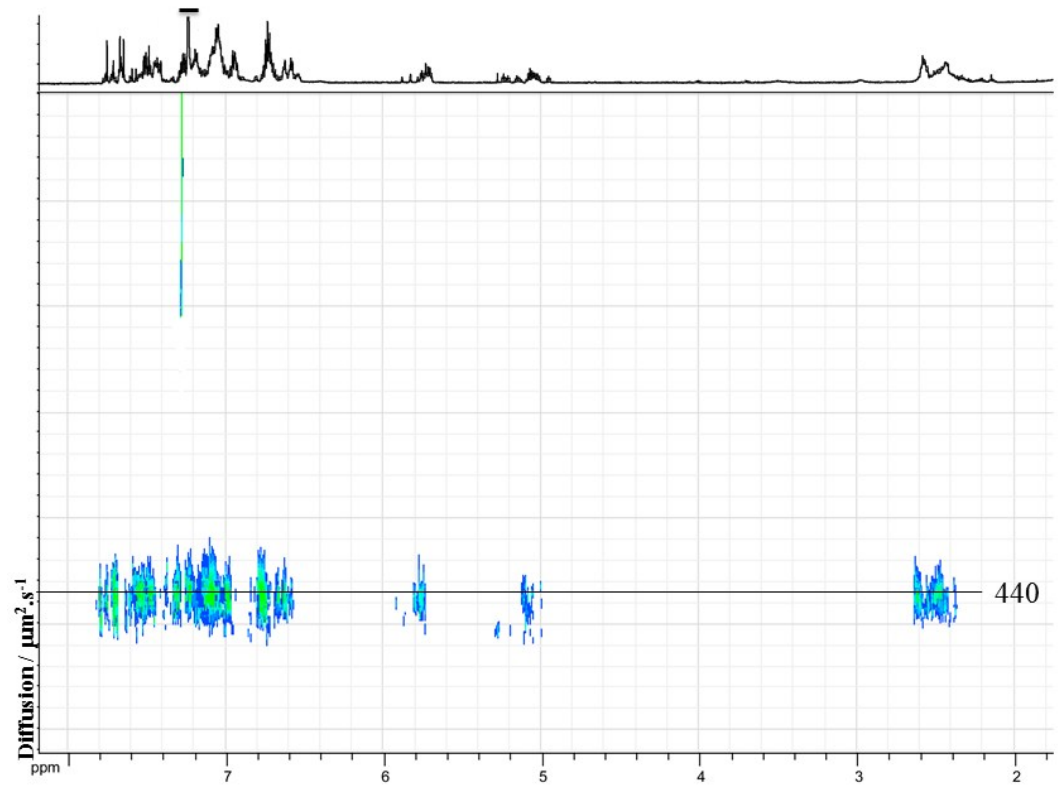


Fig 8: ¹H NMR DOSY map (CDCl_3) of $[\text{Ti}(\text{L}^2)_2(\text{DHA})_4]$.

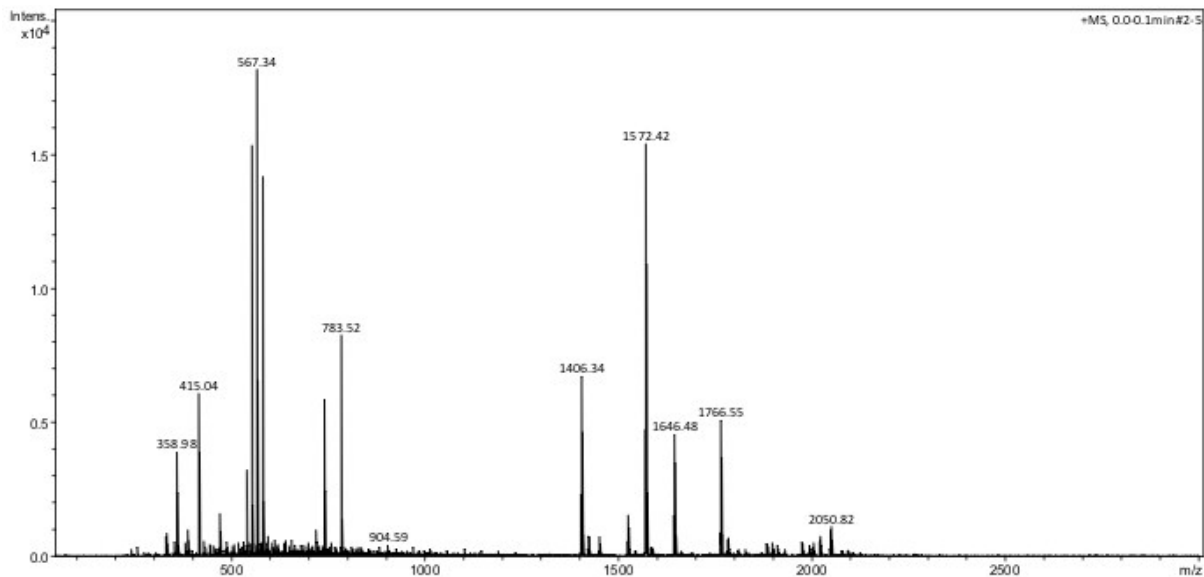


Fig 9: ES-MS spectrum of $[\text{Ti}(\text{L}^2)_2(\text{DHA})_4]$.

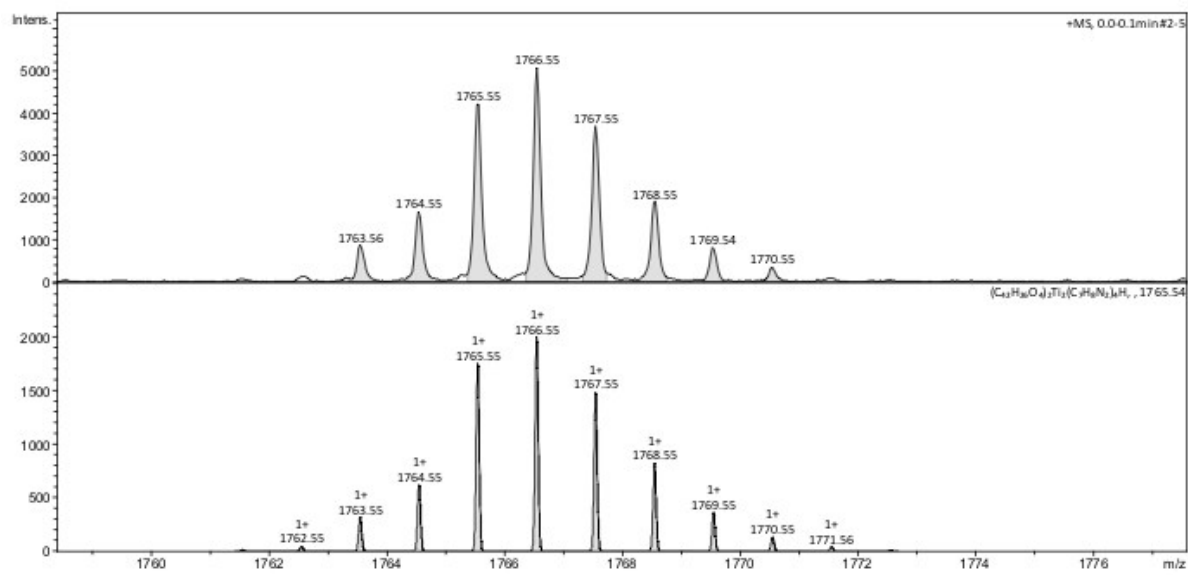


Fig 10: ES-MS spectrum of $[Ti(L^2)_2(DHA)_4]$. Enlargement at $m/z = 1766$. Experimental peak (top) and simulated peak for $[Ti(L^1)_2(DHA)_4] + H^+$ (bottom).

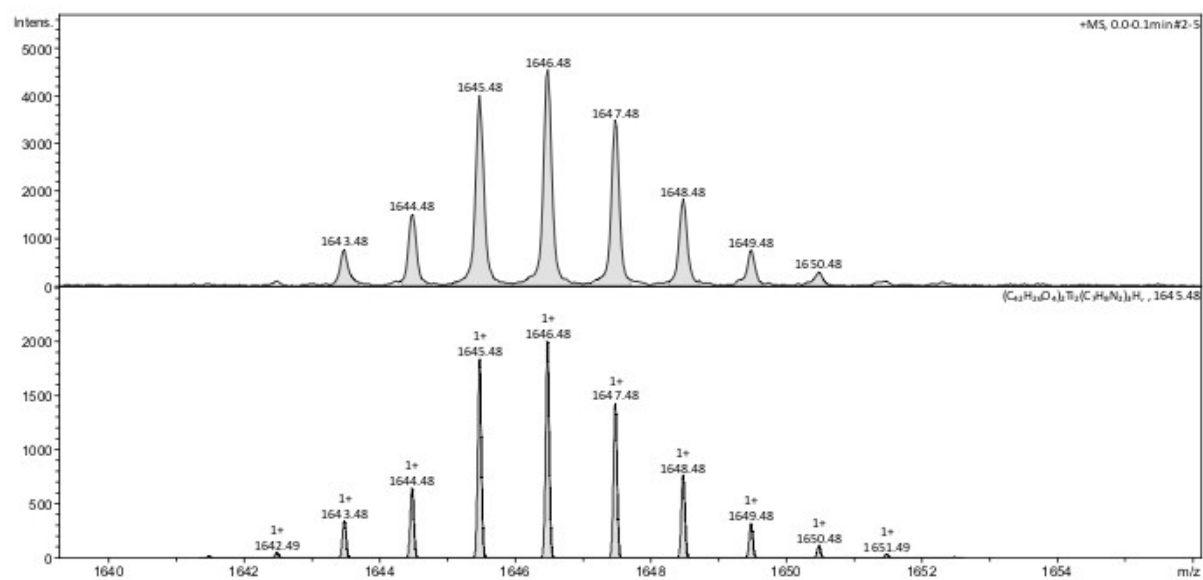


Fig 11: ES-MS spectrum of $[Ti(L^2)_2(DHA)_4]$. Enlargement at $m/z = 1646$. Experimental peak (top) and simulated peak for $[Ti(L^1)_2(DHA)_3] + H^+$ (bottom).

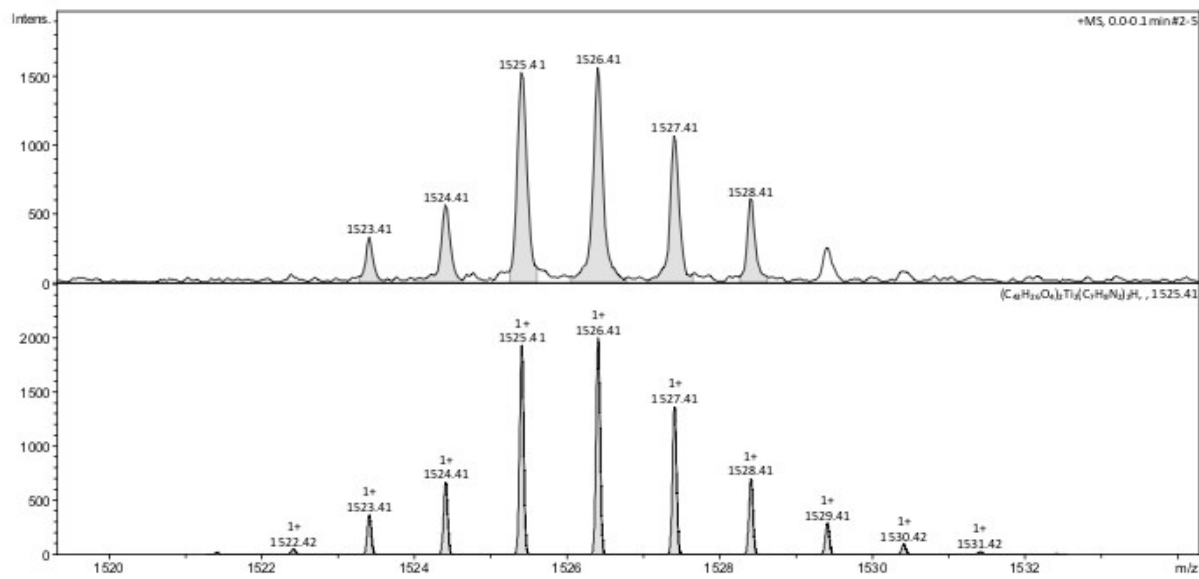


Fig 12: ES-MS spectrum of $[\text{Ti}(\text{L}^2)_2(\text{DHA})_4]$. Enlargement at $m/z = 1525$. Experimental peak (top) and simulated peak for $[\text{Ti}(\text{L}^1)_2(\text{DHA})_2] + \text{H}^+$ (bottom).

IR spectra, DHA, $[\text{Ti}(\text{L}^1)_2(\text{DHA})_2]$, $[\text{Ti}(\text{L}^2)_2(\text{DHA})_4]$

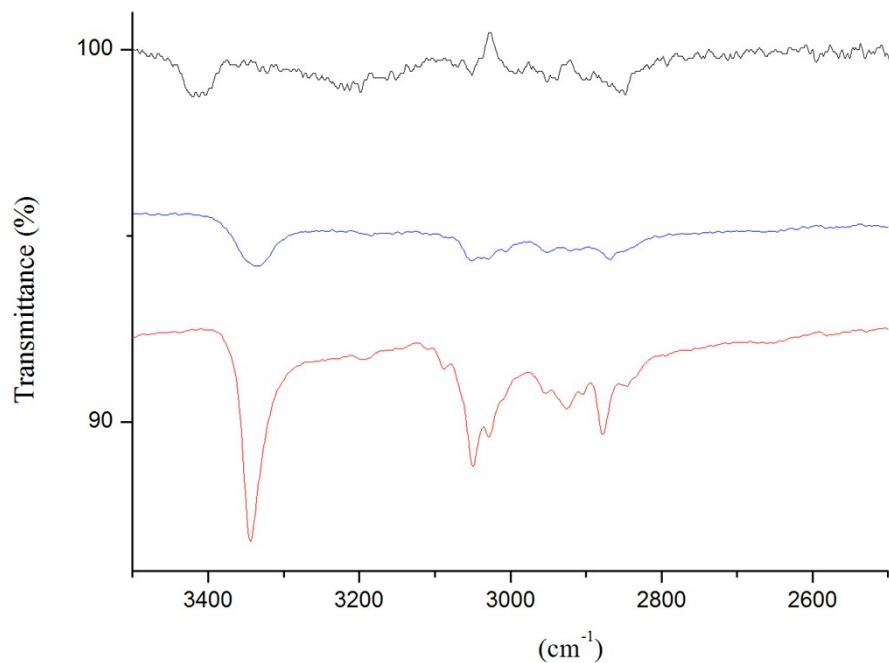


Fig 13: Infra-red spectra (region between 3500 cm^{-1} and 2500 cm^{-1}) of DHA (0.1 M in toluene) (black curve), $[\text{Ti}(\text{L}^1)_2(\text{DHA})_2]$ (blue curve) and $[\text{Ti}(\text{L}^2)_2(\text{DHA})_4]$ (red curve).

IR spectra: MePyr, $[\text{Ti}(\text{L}^1)_2(\text{MePyr})_2]$, $[\text{Ti}(\text{L}^2)_2(\text{MePyr})_4]$

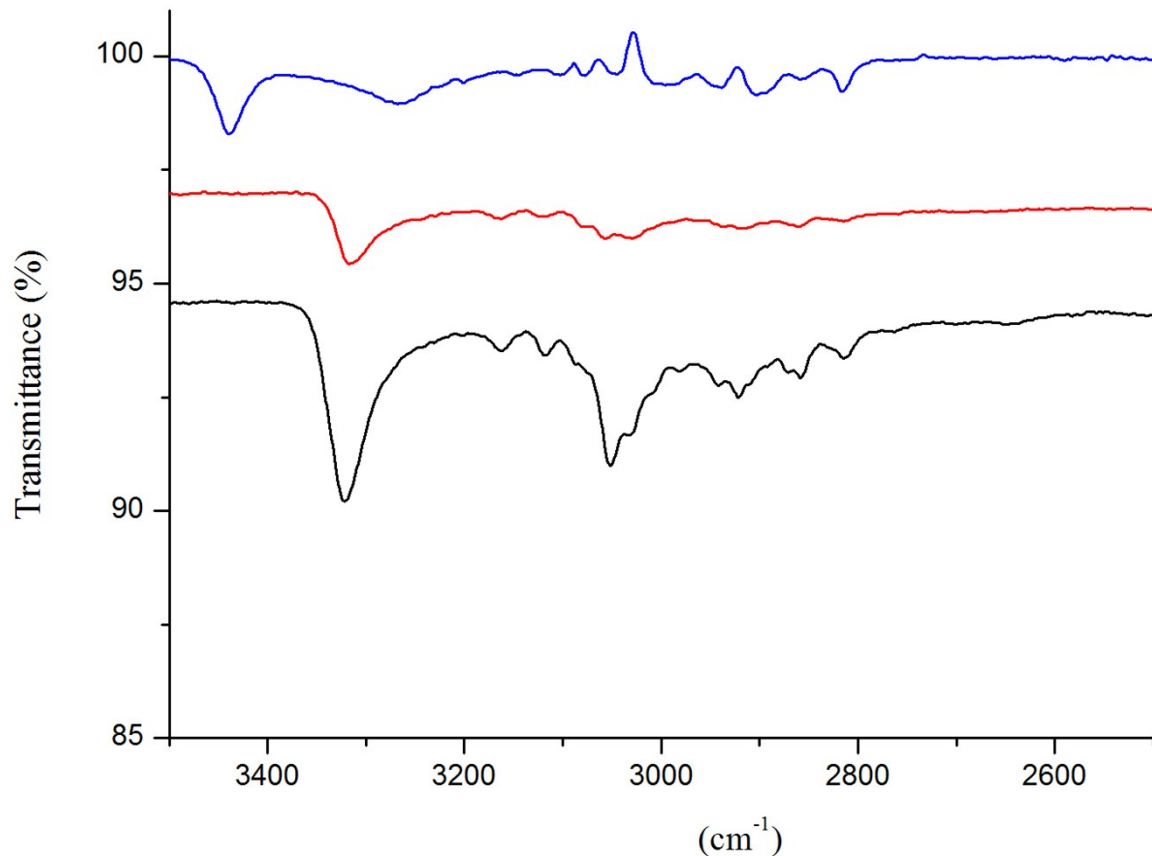


Fig 14: Infra-red spectra (region between 3500 cm^{-1} and 2500 cm^{-1}) of MePyr (0.1 M in toluene) (blue curve), $[\text{Ti}(\text{L}^1)_2(\text{MePyr})_2]$ (red curve) and $[\text{Ti}(\text{L}^2)_2(\text{MePyr})_4]$ (black curve).

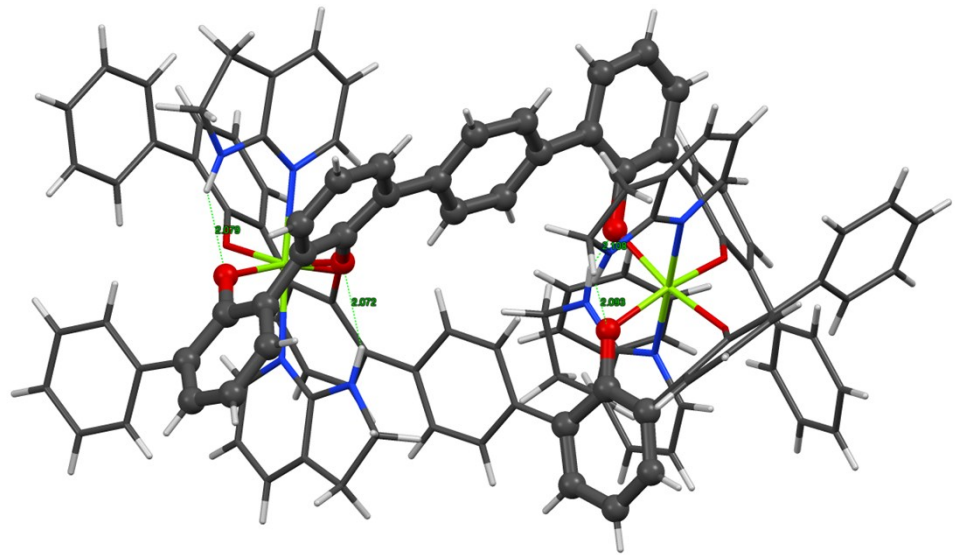


Fig 15: View of the molecular structure of $[\text{Ti}(\text{L}^1)_2(\text{DHA})_2]$ evidencing the helicity of one strand and the intramolecular inter-ligand hydrogen-bonding $\text{NH}\bullet\bullet\bullet\text{O}$ interactions.

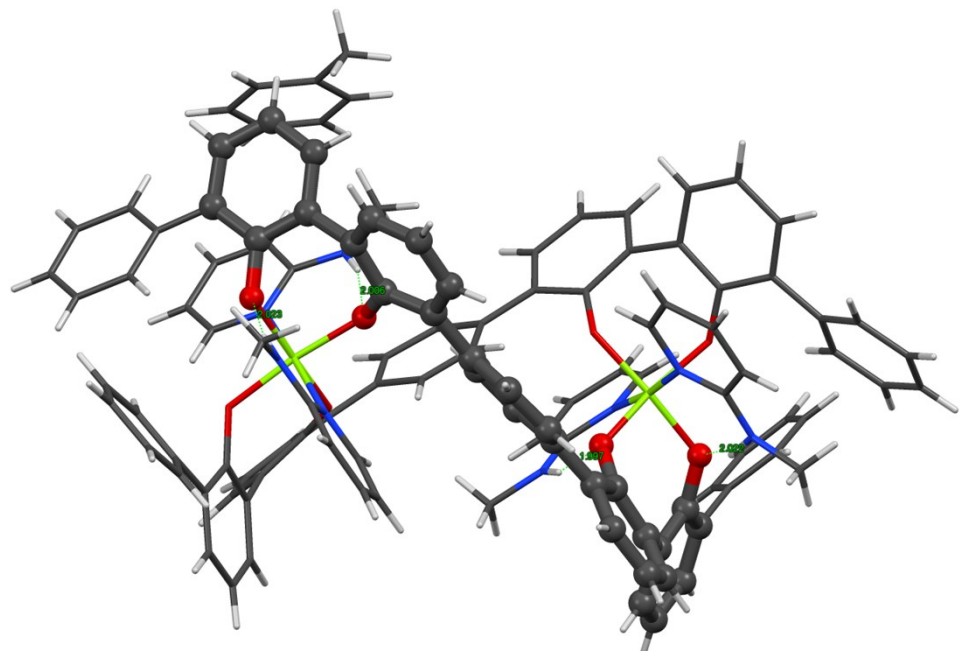


Fig 16: View of the molecular structure of $[\text{Ti}(\text{L}^1)_2(\text{MePyr})_2]$ evidencing the helicity of one strand and the intramolecular inter-ligand hydrogen-bonding $\text{NH}\bullet\bullet\bullet\text{O}$ interactions.